OFFICE OF NAVAL RESEARCH

GRANT or CONTRACT: N00014-91J-0201

R&T CODE: 4133032
Robert J. Nowak

TECHNICAL REPORT NO. 47

by Vinod P. Menon, Junting Lei and Charles R. Martin

Prepared for Publication

in Chemistry of Materials

Colorado State University
Department of Chemistry
Fort Collins, CO 80523-1872

**********End page 1

DISCLAIMER NOTICE

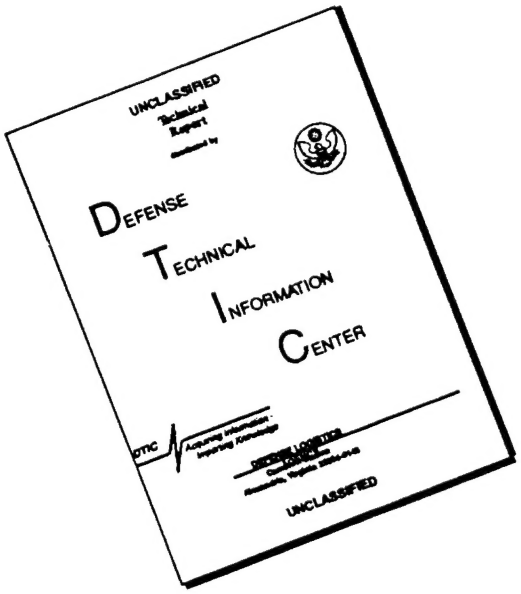

THIS DOCUMENT IS BEST QUALITY AVAILABLE. THE COPY FURNISHED TO DTIC CONTAINED A SIGNIFICANT NUMBER OF PAGES WHICH DO NOT REPRODUCE LEGIBLY.

REPORT DOCUMENTATION PAGE

2. June 6, 1996

3. Interim report

4. "Investigation of Molecular and Supermolecular Structure in Template-Synthesized Polypyrrole Tubules and Fibrils"

5. GRANT: N00014-91J-0201, R&T CODE: 4133032

6. Vinod P. Menon, Junting Lei and Charles R. Martin

7. Charles R. Martin, Department of Chemistry, Colorado State University, Fort Collins, CO 80523-1872

8. TECHNICAL REPORT NO. 47

9. Office of Naval Research, Chemistry Division, 800 North Quincy Street, Arlington, VA 22217-5660

11. To be published in Chemistry of Materials

13. Abstract: Nanotubules and nanofibrils of polypyrrole were chemically synthesized using the pores of nanoporous polycarbonate membrane filters as templates. We have previously shown that such "template-synthesized" nanofibrils of polypyrrole can have enhanced conductivities relative to more conventional forms of the polymer (e.g., thin films). Furthermore, we have shown that this enhancement in conductivity is critically dependent on the diameter of the nanofibrils; the narrowest diameter fibrils show the greatest enhancements in conductivity. In this paper, we explore the genesis of this enhancement in conductivity by determining the relative conjugation lengths in the polypyrrole fibrils using FTIR and UV-Visible-NIR spectroscopies. Using polarized infrared absorption and FTIR spectroscopies, we have followed the evolution of polymer chain orientation and conjugation length with polymer chain growth on the pore walls of the template membrane. On the basis of these results, we have proposed a bilayer model to explain the enhancement in conductivity and its strong dependence on fibril diameter.

14. Subject terms: Nanomaterials, conductive polymers, nanostructures

17. 18. 19. Unclassified

Investigation of Molecular and Supermolecular Structure in Template-Synthesized Polypyrrole Tubules and Fibrils.

Vinod P. Menon, Junting Lei, and Charles R. Martin*

Department of Chemistry, Colorado State University

Fort Collins, CO 80523

*Corresponding Author

ABSTRACT

Nanotubules and nanofibrils of polypyrrole were chemically synthesized using the pores of nanoporous polycarbonate membrane filters as templates. We have previously shown that such "template-synthesized" nanofibrils of polypyrrole can have enhanced conductivities relative to more conventional forms of the polymer (e.g. thin films). Furthermore, we have shown that this enhancement in conductivity is critically dependent on the diameter of the nanofibrils; the narrowest diameter fibrils show the greatest enhancements in conductivity. In this paper, we explore the genesis of this enhancement in conductivity by determining the relative conjugation lengths in the polypyrrole fibrils using FTIR and UV-Visible-NIR spectroscopies. Using polarized infrared absorption and FTIR spectroscopies, we have followed the evolution of polymer chain orientation and conjugation length with polymer chain growth on the pore walls of the template membrane. On the basis of these results , we have proposed a bilayer model to explain the enhancement in conductivity and its strong dependence on fibril diameter.

INTRODUCTION

We have been investigating the concept of using the pores in nanoporous membranes as templates for the synthesis of nanomaterials[1,2] This method yields monodisperse nanoscopic fibrils and tubules of the desired material. This approach is called "template-synthesis" because the pores in the membrane are used as templates to prepare the nanostructures. We have previously shown that template-synthesized electronically conductive polymer nanofibrils can have electronic conductivities that are orders of magnitude higher than conventional forms (e.g. powders or thin films) of the same polymer.[3-6]

In this paper, we explore the genesis of this enhancement in conductivity and its dependence on fibril diameter. Using a variety of experimental techniques including electron microscopy, polarized infrared absorption spectroscopy, conventional FTIR spectroscopy, DC conductivity, and UV-Vis-NIR spectroscopy, we show that in addition to enhanced polymer chain orientation,[3,4] the narrowest diameter fibrils have enhanced conjugation lengths. By following the evolution of the conjugation length and the degree of polymer chain orientation with polymer growth, we propose a simple bilayer model to explain the strong dependence of polymer conductivity on fibril diameter.

EXPERIMENTAL SECTION

Materials. Pyrrole (Aldrich, 99%) was distilled under nitrogen, immediately prior to use. Purified water, obtained by passing house-distilled water through a Milli-Q (Millipore) water purification system, was used to make all solutions. Ferric chloride, para-toluenesulfonic acid and anhydrous methanol were used as received. Poretics microporous polycarbonate membrane filters (Poretics Corp.) were used as the template membranes. These membrane filters are available in a variety of pore sizes and pore densities. The specifications of the membranes used in these studies are shown in Table I .

Polymer Synthesis. Polypyrrole (PPy) was synthesized chemically using $FeCl_3$ as the oxidizing agent. In our previous investigations, polymerizations were carried out by allowing the template membrane to separate an aqueous solution of the monomer from an aqueous solution of the oxidizing agent.[3,4] We have since developed an easier method, based on the work of Kuhn et al.[7] The template membrane was immersed into an aqueous solution that was 0.2 M in pyrrole, and an equal volume of oxidant solution (0.5 M $FeCl_3$ and 0.5 M para-toluenesulfonic acid, pTSA) was added. It has been shown that the addition of pTSA to the polymerization solution causes preferential incorporation of the sulfonate as the dopant ion.[5,8,9] The mixture was allowed to polymerize at room temperature for the desired length of time. No effort was made to exclude oxygen during polymerization. PPy preferentially nucleates and grows on the pore walls.[3,4] As a result, PPy tubules are formed at short polymerization times; polymerization times of 1 hr. resulted in solid PPy fibrils.

To investigate the effects of synthesis temperature on conductivity, some fibrils were synthesized at low temperatures (0°C and -20°C). A 50:50 $MeOH/H_2O$ mixture was used as the solvent for these syntheses, and polymerizations were allowed to proceed for 6 to 12 h.

For some experiments, it was desirable to free and collect the tubules that were prepared in the pores of the template membrane. This was done by dissolving the polycarbonate template in dichloromethane, after removing the PPy surface layers that coat both faces of the membrane.[3,4] The surface layers were removed by polishing the faces with 1 μm alumina powder. The membrane was then ultrasonicated in water to remove the alumina powder. The PPy tubules were collected by filtration on an alumina filter,[10,11] and then repeatedly rinsed with dichloromethane to remove traces of polycarbonate.

Electron Microscopy. Scanning electron microscopic (SEM) images were obtained using a Phillips 505 microscope. The PPy tubules were sputtered with a thin film of gold prior to imaging. Transmission electron microscopy (TEM) was carried out using a JEOL 2000 scope. TEM samples were prepared as follows: The surface layers were removed as described above, and a small (0.1 cm^2) piece of the template membrane (with the PPy tubules inside the pores) was held under vacuum on a Cu TEM grid (200 mesh, Ted Pella Inc.). The membrane was then dissolved using chloroform followed by dichloromethane, leaving the PPy tubules on the grid. Chloroform was used first because it is a less aggressive solvent for the dissolution of polycarbonate. As a result, the tubules are not dispersed or rinsed from the grid.

Polarized Infrared Absorption Spectroscopy (PIRAS). PIRAS can be used to study the extent of polymer chain orientation in template-synthesized conductive polymers.[4,6,10] Data were obtained using a Mattson Galaxy Fourier transform infrared spectrometer. The polarizations used are shown in Figure 1.[4] An Al wire grid polarizer was used to control polarization. The polarization $I_{\perp}$ is orthogonal to the axes of the PPy tubules (though we use the term tubules in this discussion, the arguments are equally valid for fibrils). The integrated absorbance by the PPy tubules of this polarization is labeled $A_{\perp}$. The polarization vector for the beam labeled I_{30} makes an angle of 30° with respect to the tubule axis, and its integrated absorbance is A_{30}. A_{30} has a component in the parallel direction and is, therefore, related to $A_{||}$, where $A_{||}$ is the integrated absorbance intensity for a beam polarized parallel to the tubule axis.

The dichroic ratio, defined as $R= A_{||} / A_{\perp}$, quantitatively describes the polymer chain orientation.[12,13] In general, R=1 implies no preferred orientation of the polymer chains. A value of R that deviates from unity shows that there is some preferred polymer chain orientation. A_{30} is related to $A_{||}$ and $A_{\perp}$via[12,13]

$$A_{30} = A_{||} \cos^2(30^\circ) + A_{\perp} \sin^2(30^\circ) \qquad (1)$$

Dividing both sides of Equation 1 by $A_{\perp}$ and rearranging yields

$$R = A_{||} / A_{\perp} = 1/3\,(4\,A_{30}/A_{\perp} - 1) \qquad (2)$$

Spectra for the PPy tubules were obtained by subtracting the spectrum due to the polycarbonate from the spectrum of the polypyrrole/polycarbonate (PPy/PC) composite membrane . This method is described in detail in a previous paper.[6] Briefly, prior to the synthesis of the PPy tubules, the template membrane was mounted in the FTIR sample holder, and background spectra were obtained for the two different polarizations shown in Figure 1. These spectra showed strong IR bands for polycarbonate. The PPy tubules were then synthesized in the pores of the template membrane as described above. The membrane was retained in the sample holder during tubule synthesis. This was done to ensure that spectra were obtained, after polymerization, on the same portion of the membrane as was used to obtain the spectra before polymerization.

After synthesis, the surface PPy layers were removed by polishing with alumina, and the membrane was cleaned with water and placed back in the spectrometer. Spectra were again recorded for the two polarizations in Figure 1. Subtraction of the corresponding background spectra yielded PPy spectra for the two polarizations.[6] The PPy bands at 1560 and 1480 cm^{-1} were used for these studies. These bands correspond to the antisymmetric and symmetric ring stretching modes for PPy, respectively.[14,15] The relative intensities of these bands is proportional to the conjugation length of PPy.[16] The evolution of the PPy spectrum was studied as a function of polymerization time by taking PIRAS data at polymerization times ranging from 5 to 300s.

X-Ray Photoelectron Spectroscopy (XPS). XPS data were obtained using a Hewlett-Packard 5950 ESCA spectrometer with monochromatized Al/Kα

radiation. The energy resolution was about 0.9 eV. Data were obtained for both PPy fibrils and bulk PPy powder. Samples were mounted on Cu sample holders using double-sided Scotch tape. The flood gun was switched off for all the measurements since the oxidized PPy samples are sufficiently conductive to prevent electrostatic charging.

Other Spectroscopic Studies. Conventional FTIR transmission mode experiments (i.e. with unpolarized radiation) were also conducted on the PPy-containing membranes. As per the PIRAS studies, the evolution of the PPy spectrum was studied as a function of polymerization time. Finally, UV-Vis-NIR spectra were obtained on the 30 nm pore-diameter PPy/PC composites as a function of the synthesis temperature. These spectra were obtained using a Hitachi U3501 spectrometer.

DC Conductivity. DC conductivity data were obtained from resistance measurements along the fibril axes of the PPy/PC composites using a two-probe method.[4] Resistance measurements were made on the PPy/PC composite membrane with the surface layers intact, and a pressure of ca. 7×10^3 psi was applied to the upper electrode during the measurement.[4] At such pressures, the contact resistance is decreased to a negligible value.[4]

RESULTS AND DISCUSSION

Electron Microscopy. Transmission electron micrographs (TEMs) of the template-synthesized PPy nanostructures obtained after dissolution of the PC template membrane are shown in Figure 2. The nanostructures in Figures 2A and 2B were obtained for polymerization times of 30 and 300 s, respectively. After short polymerization times, a thin-walled PPy tubule is obtained within each pore(Figure 2A). As the polymerization time increases, polymer grows inwards from the pore wall leading to increased tubule wall thickness (Figure 2B). This

increase in wall thickness makes the walls appear darker in Figure 2B. Further polymerization causes the tubules to close up forming solid PPy fibrils.[4]

Striations are observed on the sides of the PPy nanotubules (Figure 2B). These striations are shown more clearly in the scanning electron micrograph in Figure 3. The pore walls of the template membrane show similar striations.[6] We believe that the striations on the pore wall result because the polycarbonate membrane is stretched during processing. Stretching aligns the polycarbonate chains in the stretch direction and induces crystallinity in the polymer.[17] The formation of such a crystalline phase would also produce changes in the FTIR spectrum of the polymer.[13] These changes have been observed in the PIRAS spectra of the stretched polymer,[6] and are consistent with the transition of the polycarbonate from a relatively amorphous to a semi-crystalline material.[13] This stretch alignment strongly influences chain orientation in the PPy synthesized within the pores of these membranes (see below).

Polarized Infrared Absorption Spectroscopy. We have previously shown that large diameter PPy fibrils (400 and 600 nm) absorb both the perpendicular and 30° polarizations to the same extent.[4] Consequently, large diameter fibrils show a dichroic ratio of unity, indicating that there is no preferred spatial orientation of the polymer chains in these fibrils.[4] In contrast, small diameter fibrils (50 and 30 nm) preferentially absorb the perpendicular polarization and have non-unity dichroic ratio.[4] This indicates a preferred spatial orientation of the polymer chains in the small diameter fibrils. The degree of chain alignment was found to be greatest in the narrowest diameter (30 nm) fibrils.[4]

In order to explore the genesis of this preferential chain orientation, we have carried out PIRAS studies on PPy synthesized in a large pore diameter (400 nm) membrane as a function of polymerization time. Recall from the TEM results (Figure 2) that control of polymerization time results in tubules having the

same outer diameter but different wall thicknesses. PIRAS data for polypyrrole tubules synthesized for various polymerization times are shown in Figure 4. The extent of dichroism for tubules polymerized for a brief time (thin-walled tubules) is high, indicating that the polymer chains in these thin-walled tubules are highly oriented. However, as polymerization time increases (i.e. wall thickness increases), the extent of dichroism decreases (Figures 4A vs. 4D).

A plot of the dichroic ratio versus polymerization time (Figure 5) shows that pronounced dichroism is observed at short polymerization times but that the extent of dichroism decreases at long times, finally reaching a value of unity. The latter result is in accord with our earlier studies that showed no preferred spatial orientation for 400 nm diameter PPy fibrils.[4] The data in Figures 4 and 5 show that the PPy deposited directly on the pore wall (short polymerization time) is highly ordered. However, as the polymerization time increases, the polymer that is subsequently deposited becomes progressively disordered. We have observed a similar effect for template-synthesized polyaniline tubules[6] and for polypyrrole films that are synthesized at electrode surfaces.[18]

While the PIRAS data clearly show that the polymer chains in these tubules are partially aligned, these data do not tell the direction of alignment. Two limiting cases - parallel and perpendicular to the axis of the tubules - are possible (Figure 6). If the angle that the transition moment for the absorption makes relative to the chain is known, then we can distinguish between these two cases. Prior investigations on thin PPy films grown on stretch-oriented PTFE tape have shown that the transition moments for the 1560 and 1480 cm^{-1} bands of PPy are directed parallel to the polymer chain axis.[19]

When dichroism is observed, it is always the perpendicular mode that is preferentially absorbed (Figure 4). Because the transition moment for these vibrations is parallel to the polymer chain, these data unequivocally show that the

polymer chains in these tubules are preferentially oriented perpendicular to the tubule axes. As indicated in the electron microscopy section, we believe that this perpendicular orientation results because the polycarbonate chains along the pore wall of the template membrane are similarly oriented.

These PIRAS data provide an explanation for the previously observed enhancement in PPy chain orientation in narrow diameter solid PPy fibrils.[4] We have found that only the layer of PPy deposited on the pore wall is oriented. This means that the solid fibrils consist of a thin outer skin of oriented material surrounding a solid inner core of disordered PPy. In the smallest diameter fibrils, the proportion of polymer chains in the oriented surface skin is significant relative to the proportion of polymer in the disordered core (Figure 7); as a result dichroism is observed in the small diameter fibrils.[4] In contrast, the vast majority of the polymer chains in the large diameter fibrils is in the disordered core (Figure 7); as a result the dichroic ratio for these large diameter fibrils is unity.[4]

Transmission FTIR spectroscopy. The electronic properties of conductive polymers are strongly dependent on conjugation length. Defects that interrupt conjugation include sp^3 carbons, carbonyl groups, cross-links etc.[16] We have recently developed an infrared spectroscopic method for obtaining a qualitative measure of the conjugation length in polypyrrole.[16] This method is based on the theoretical work by Tian and Zerbi.[14,15] We have used this method here to explore conjugation lengths in our template-synthesized PPy solid fibrils as a function of fibril diameter and synthesis temperature.

Tian and Zerbi have used a parameter called the effective conjugation coordinate to calculate IR spectra for PPy.[14,15] This theory successfully predicts the number and position of the main infrared bands of PPy and shows that the IR spectrum is strongly influenced by the conjugation length. In particular, Zerbi's calculations predict that as the conjugation length is increased, the intensity of

the antisymmetric ring stretching mode at 1560 cm^{-1} will decrease relative to the intensity of the symmetric mode at 1480 cm^{-1}.[14,15] As a result, the ratio of the intensities of the 1560 cm^{-1} and 1480 cm^{-1} bands in an experimental IR spectrum can be used to obtain a relative measure of the conjugation length.[16]

Figure 8 shows that the intensities of the 1560 and 1480 cm^{-1} bands for the PPy fibrils are strongly dependent on fibril diameter. These data were quantified by ratioing the integrated absorption intensities for these bands (A_{1560}/A_{1480}). The A_{1560}/A_{1480} ratio for solid PPy fibrils of various diameters are shown in Table II. These data show that as the fibril diameter decreases, the conjugation length of the PPy that makes up the fibril increases (lower value of A_{1560}/A_{1480}). The DC conductivities of the various fibrils are also shown in Table II. As would be expected,[4,20,21] the conductivity increases with conjugation length, and the narrowest diameter fibrils are most conductive.

We have recently shown that A_{1560}/A_{1480} is linearly related to the log of the DC conductivity for conventional chemically-synthesized polypyrrole.[16] This is not surprising since both A_{1560}/A_{1480} and the DC conductivity are critically dependent on conjugation length.[20,21] Figure 9 shows a plot of A_{1560}/A_{1480} vs. the log of the DC conductivity for template-synthesized PPy fibrils of different diameters. In accordance with our earlier experiments on chemically-synthesized PPy powders,[16] we find that the log of the conductivity in our template-synthesized PPy is linearly related to A_{1560}/A_{1480}.

PPy synthesized at low temperatures typically shows higher conductivity than room-temperature-synthesized material.[3,4,22,23] We have previously shown that this applies for template-synthesized PPy fibrils as well.[3,4] We explore this issue here by using the A_{1560}/A_{1480} method to investigate the relative conjugation lengths in 30 nm-diameter PPy fibrils synthesized at three different temperatures (Figure 10). The relative intensities of the ring stretching bands

show that the low temperature fibers have extended conjugation. The conductivity and A_{1560}/A_{1480} data for these fibrils are shown in Table III. Note that in agreement with the preceding data and with Zerbi's theory,[14,15] the fibers with the highest conductivity have the lowest value of A_{1560}/A_{1480}.

It is interesting to note that the DC conductivity values reported here were obtained in a direction perpendicular to the direction of polymer chain orientation ($\sigma_{\perp}$).[4] Our data show that, as expected,[20] $\sigma_{\perp}$ increases with conjugation length (as would the conductivity parallel ($\sigma_{\parallel}$) to the chain orientation direction). We have seen analogous enhancements in conductivity in thin films prepared from template-synthesized tubules, in which the tubule axes are randomly oriented[5,6] The most interesting prospect, however, would be to obtain a direct measurement of $\sigma_{\parallel}$ in the template-synthesized materials. This could be accomplished if a thin film in which the tubule axes are aligned parallel to each other could be obtained. $\sigma_{\parallel}$ would then be the conductivity in a direction perpendicular to the aligned tubule axes. We are currently attempting to prepare such aligned thin-film samples.

To explore the genesis of the enhanced conjugation in the smallest diameter fibrils, A_{1560}/A_{1480} values were obtained for PPy synthesized in a large pore-diameter (400 nm) membrane as a function of polymerization time (Figure 11). At short polymerization times (thin walled tubules), the intensities of the 1560 and 1480 cm^{-1} bands are comparable, indicating extended conjugation. With an increase in the tubule wall thickness, however, the intensity of the 1560 cm^{-1} band increases relative to the 1480 cm^{-1} band, indicating a decrease in the conjugation length. Figure 12 shows the corresponding plot of A_{1560}/A_{1480} vs. polymerization time. These data show that the layer of polymer deposited on the pore wall (short polymerization time) has extended conjugation, but that the conjugation length decreases in the subsequently-deposited layers. Hence the

PIRAS and A_{1560}/A_{1480} methods tell a consistent story about the template-synthesized materials.

Finally, it is worth noting that Gregory et al. have deposited thin films of PPy onto various fabrics.[7] In analogy to our work, they found that the surface-grown PPy has extended conjugation, and that the higher conjugation length can be attributed to a lower number of α-β (conjugation-interrupting) linkages.[7] Apparently, the surface forces the pyrrole monomers to be co-planar during bond formation. This planar configuration favors α–α linkage.

UV-Visible-NIR Spectroscopy. Figure 13 shows optical spectra for 30 nm-diameter PPy fibrils synthesized at three different temperatures. In agreement with previously observed results,[16,24,25] these spectra show two distinct bands - one centered at ~500 nm and the other at ~1300 nm. According to Bredas and Street,[25] and Bredas et al.,[24] these transitions result because fully doped PPy contains a bipolaron and an antibipolaron band within the band gap. The low energy band in the optical spectrum of PPy is due to electronic transitions between the valence band and the bipolaron band, and the high energy band is due to transitions between the valence band and the antibipolaron band.

The most obvious trend in the absorption spectra shown in Figure 13 is the red-shift in the peak positions with decreasing synthesis temperatures. This is particularly obvious in the low-energy transition, where the peak maximum shifts from 1240 nm in the PPy fibrils synthesized at 25°C to 1425 nm in the fibrils synthesized at -20°C. We have shown previously[16] that a red-shift in the peak positions corresponds to a decrease in the bandgap which is a direct consequence of an increase in the conjugation length. Hence these data support the general observation that the effective conjugation length in PPy increases with a decrease in synthesis temperature.

Finally, it is pertinent to add that the maximum absorbance (in the near IR region) is highest for fibrils synthesized at the lowest temperature (Figure 13). Since the free carriers in PPy are responsible for both its absorbance in the near-IR region[16] as well as its electronic conductivity, it is not surprising that the most highly electronically conducting fibrils also have the highest absorbance. Once again, these data corroborate the conclusion drawn from the FTIR data - polymer chains with extended conjugation exhibit higher conductivities.

X-Ray Photoelectron Spectroscopy.

Core level C1s XPS spectra. Figure 14 shows the C1s spectra for 30 nm-diameter PPy fibrils and for bulk PPy powder. As was observed in the pioneering work by the IBM group, these spectra are asymmetric and can be deconvolved into a series of component Gaussian peaks.[26] A standard lineshape analysis using the spectrometer's Gaussian-fitting program reveals that the C1s spectrum for the bulk sample can be deconvolved into four peaks (maxima at 283.7, 284.9, 286.1, and 287.7 eV); the C1s spectrum for the fibrillar sample can be deconvolved into only three peaks (284.3, 285.9, and 287.9 eV) (Table IV).

The difference between the C1s spectra for the fibrillar and bulk-powder samples is the absence of the lowest binding-energy peak (283.7 eV) in the fibrillar sample (Figure 14, Table IV). For this reason, we focus our attention on the low bonding-energy wings of the spectra. The high binding-energy wings (which are essentially identical for the fibrillar and powder samples) have been discussed by Street[26] and by us.[22] For example the ~288 eV peak has been assigned to carbonyl defects.[22] The data in Table IV show that both the fibrillar and powder PPy samples contain very low concentrations of carbonyl defects.

In pyrrole monomer, the presence of the nitrogen atom creates different chemical environments for the α and β carbons and this leads to an energy splitting in the low binding energy wing of the C1s signal.[27] A similar splitting has

been observed by us (Figure 14b) and others[26,28-30] for bulk PPy. However, as indicated in our bulk-powder spectrum, the intensities of the α and β carbons peaks are not the same. Street has discussed the reasons for this difference in peak intensity.[26] The splitting of the α and β carbons peaks in the bulk-powder PPy sample indicates that like pyrrole monomer,[27] the chemical environments of the α and β carbons are different in the bulk powder. We have recently shown that in the bulk PPy powder, the positive charge of the doped material resides predominantly on the N.[16,22] Because the α C is directly bonded to this N^+, whereas the β C is an atom removed from this N^+, the chemical environments for the α and β Cs are not the same. This explains the splitting of the α and β C peaks in the bulk powder (Figure 14b).

The C1s spectrum for the fibrillar sample (Figure 14a) shows that the chemical environments of the α and β Cs in this sample are essentially the same. This, in fact, would be the expected result if conjugation is extended in fibrillar PPy, as the preceding results have shown. This is because the consequence of the extended conjugation is delocalization of the positive charge of the doped material. That is, rather than being localized to the N of a single ring, the positive charge in the fibrillar sample is delocalized over the atoms in several rings. As a result of this spreading out of the positive charge, the chemical environments for both carbons are essentially the same, and the C1s signal is no longer split into separate α and β C peaks. Hence, the C1s XPS data support our assertion that conjugation is extended in the fibrillar material.

Core level N1s XPS spectra. Figure 15 shows typical N1s core level spectra for the fibrillar and bulk PPy samples. Like the C1s signal, the lineshape of the N1s signal is quite asymmetric. For both the bulk-powder and fibrillar samples, the N1s spectra are dominated by a peak at ~399.7 eV. This main peak has been assigned to neutral (i.e. uncharged) nitrogen atoms in the polymer.[28] In addition,

to this main peak, a shoulder appears at low binding energy (~397.6 eV). Skotheim et al. assigned this low binding energy shoulder to deprotonated, uncharged imine nitrogen atoms.[31] We have used this peak to assess the concentration of such imine-defects in bulk PPy samples prepared at various synthesis temperatures.[22] The relative abundance of this peak (Table IV) in the bulk-powder sample (13.9%) and in the fibrillar sample (4.6 %) indicates that there are fewer of these imine defects in the fibrillar sample. Since imine defects interrupt conjugation,[22] a lower concentration of such defects would be expected, given the extended conjugation of the fibrillar material.

Two high-energy shoulders are also observed (Figure 15). Eaves et al. proposed that these high binding energy peaks are due to nitrogen atoms that bear a unit positive charge and are in chemically or structurally inequivalent environments.[32] This assignment is supported by the observation that the area of these high binding-energy peaks correlates with the doping level of the polymer.[16,22,31-33] For example, we have used the ratio of the areas of the ~401 eV and ~400 eV peaks to determine the doping level of PPy.[16,22] We have called this ratio the N^+/N ratio to indicate it relationship to the doping level.[16,22]

This ability to correlate the N^+ signal in the N1s XPS spectrum to the doping level is predicated on the idea that the positive charge is localized to a fraction (e.g. 1/3 for a 33% doped polymer) of the N atoms in the polymer. Put another way, for every dopant anion in the polymer there is a corresponding N^+ to which this anion is electrostatically bound. We have established, however, that the positive charge in the fibrillar material is not localized (or at least much less localized) to the N atoms. This would suggest that the relative proportion of the high binding-energy (N^+) peaks should be less in the fibrillar material than in the bulk material. Table IV shows that this is, indeed, the case.

In addition, the charge delocalization in the fibrillar material would suggest that the area of the high binding energy peaks should not correlate with doping level. To explore this idea, we obtained elemental analyses on the fibrillar and powder materials (Table V). From these analyses we find that the doping level of the powder material is 22% whereas the doping level of the fibrillar material is 32 %. The sum of the areas of the high binding-energy peaks for the fibrillar material (Table IV) represents 16% of the total N signal. Hence, in agreement with our prediction, the N^+ signal in the fibrillar material does not correlate with (and is much less than) the doping level in this material. In contrast, the sum of the areas of the high binding-energy peaks for the powder material is 23% (Table IV), and this correlates nicely with the doping level (22%, Table V).

CONCLUSIONS

Based on the evidence presented above we have developed a simple model that explains the enhancement in electronic conductivity[3,4] observed in the narrow diameter PPy fibrils. We propose that during the template synthesis, the PPy initially deposited on the pore walls is highly oriented and has extended conjugation. The orientation is derived from the templating effect of the underlying polycarbonate chains which are highly ordered due to stretch-orientation.[6] With subsequently deposited layers, this order-inducing influence of the pore wall is quickly lost and the polymer chains become randomly oriented. This idea of inducing order in a polymer film by synthesizing it on an ordered polymeric substrate has been demonstrated with other systems.[48] The template synthesized fibrils, therefore, are composed of a thin outer skin of highly oriented, large conjugation length, polymer that is highly conducting, cladding a disordered, low conjugation length core that has poor conductivity (Figure 7). The enhancement in conductivity in the narrow diameter fibrils is due to the fact that

these fibrils have a larger fraction of highly conducting polymer than the large diameter fibrils (Figure 7).

These analyses have led us to an important generalization: An increase in the supermolecular order through alignment of polymer chains also causes a molecular-level benefit - increase in the conjugation length. This is not surprising since an alignment of the polymer chains requires that the chains be relatively linear with few kinks and defects; such a linear chain would also promote extended conjugation. Finally, by improving molecular and supermolecular order in this way, we obtain materials with enhanced electronic conductivities.

Acknowledgment:. This work was supported by the Office of Naval Research.

REFERENCES

(1) Martin, C. R. *Science.* **1994**, *266*, 1961.

(2) Martin, C. R. *Acc. Chem. Res.* **1995**, *28*, 61.

(3) Cai, Z.; Martin, C. R. *J. Am. Chem.Soc.* **1989**, *111*, 4138.

(4) Cai, Z.; Lei, J.; Liang, W.; Menon, V.; Martin, C. R. *Chem. Mater.* **1991**, *3*, 960.

(5) Martin, C. R.; Parthasarathy, R.; Menon, V. *Synt. Met.***1993**, *55-57*, 1165.

(6) Parthasarathy, R. V.; Martin, C. R. *Chem. Mater.* **1994**, *6*, 1627.

(7) Gregory, R. V.; Kimbrell , W. C.; Kuhn , H. H. *Synth. Met.* **1989**, *28*, C823.

(8) Martin, C. R.; Parthasarathy, R.; Menon, V. *Electrochim. Acta* **1994**, *39*, 1309.

(9) Armes, S. P.; Aldissi, M.; Hawley, M.; Beery, J. G.; Gottesfeld, S. *Langmuir* **1991**, *7*, 1447.

(10) Liang, W.; Martin, C. R. *J. Am. Chem. Soc.* **1990**, *112*, 9667.

(11) Brumlik, C. J.; Martin, C. R. *J. Am. Chem. Soc.* **1991**, *113*, 3175.

(12) Monnerie, L. In *Developments in Oriented Polymers*; I. M. Ward, Ed.; Elsevier: London, 1987; Vol. 2.

(13) Zbinden, R. *Infrared Spectroscopy of High Polymers*; Academic Press: NY, 1964, p. 186.

(14) Tian, B.; Zerbi, G. *J. Chem. Phys.* **1990**, *92*, 3892.

(15) Tian, B.; Zerbi, G. *J.Chem. Phys.* **1990**, *92*, 3886.

(16) Lei, J. T.; Cai, Z.; Martin, C. R. *Synth. Met.* **1992**, *46*, 53.

(17) Billmeyer, F. W. In *Textbook of Polymer Science*; Wiley-Interscience Publication: New York, 1984; p. 290.

(18) Cai, Z.; Martin, C. R. *J. Electroanal. Chem.* **1991**, *300*, 35.

(19) Lei, J. T.; Menon, V. P.; Martin, C. R. *Polym. Adv. Tech.* **1993**, *4*, 124.

(20) Baughman, R. H.; Shacklette, L. W. *Phys. Rev. B* **1989**, *39*, 5872.

(21) Baughman, R. H.; Shacklette, L. W. *J. Chem. Phys.* **1989**, *90*, 7492.

(22) Liang, W.; Lei, J.; Martin, C.R. *Synth. Met.* **1992**, *52*, 227.

(23) Ogasawara, M.; Funahashi, K.; Demura, T.; T.Hagiwara; Iwata, K. *Synth. Met.* **1986**, *14*, 61.

(24) Bredas, J. L.; Scott, J. C.; Yakushi, K.; Street, G. B. *Phys. Rev.* **1984**, *30*, 1023.

(25) Bredas, J. L.; Street, G. B. *Acc. Chem. Res.* **1985**, *18*, 309.

(26) Street, G.B. in Handbook of Conductive Polymers, Vol. 1, Skotheim, T.A. Ed. Marcel Dekker, NY,1986.

(27) Clark, D. T.; Lilley, D. M. *Chem. Phys. Lett.* **1971**, *9*, 234.

(28) Pfluger, P.; Street, G. B. *J. Phys. Chem.* **1984**, *80*, 544.

(29) Hino, S.; Iwasaki, K.; Tatematsu, H.; Matsumoto, K. *Bull. Chem. Soc. Jpn.* **1990**, *63*, 2199.

(30) Ribó, J. M.; Dicko, A.; Tura, J. M.; Bloor, D. *Polymer* **1991**, *32*, 728.

(31) Skotheim, T. A.; Florit, M. I.; Melo, A.; O'Grady, W. E. *Synth. Met.* **1983**, *14*, 271.

(32) Eaves, J. G.; Munro, H. S.; Parker, D. *Polym. Commun.* **1987**, *28*, 38.

(33) Kang, E. T.; Neoh, K. G.; Ong, Y. K. *Synth. Met.* **1990**, *39*, 69.

(34) Wittmann, J. C.; Smith, P. *Nature* **1991**, *352*, 414.

FIGURE CAPTIONS

Figure 1. Experimental set-up for the PIRAS experiments.

Figure 2A. Transmission electron micrographs of polypyrrole tubules synthesized in 400nm polycarbonate membrane. Polymerization time = 30s.

Figure 2B. Transmission electron micrographs of polypyrrole tubules synthesized in 400nm polycarbonate membrane. Polymerization time = 300s.

Figure 3. Scanning electron micrograph of 400nm diameter polypyrrole fibrils.

Figure 4. PIRAS data for polypyrrole tubules of four different wall thicknesses. Outside diameter of tubules = 400nm.

Figure 5. Dichroic ratios (at 1560 cm^{-1}) for polypyrrole tubules of various wall thicknesses. Outside diameter of tubule = 400 nm. Wall thicknesses controlled by varying polymerization time.

Figure 6. Two possible orientations of the PPy chains and the transition moment relative to the fibril axis. Both orientations would yield enhanced absorbance of $I_{\perp}$, which is the experimentally observed result.

Figure 7. Proposed anatomy of template-synthesized PPy fibrils.

Figure 8. Transmission FTIR spectra of polypyrrole fibrils of the indicated diameters. The 1560 cm^{-1} and 1480 cm^{-1} bands are highlighted in these spectra.

Figure 9. Plot of the log(conductivity) vs. the ratio of the integrated absorption intensities of the 1560 cm^{-1} and 1480 cm^{-1} bands for the polypyrrole fibrils shown in Figure 8.

Figure 10. Transmission FTIR spectra of 30nm diameter polypyrrole fibrils synthesized at the indicated temperatures. The 1560 cm^{-1} and 1480 cm^{-1} bands are highlighted in the spectra

Figure 11. Transmission FTIR spectra for polypyrrole tubules of various wall thicknesses. Outside diameter of tubule = 400 nm. Wall thicknesses controlled by varying polymerization time. The 1560 cm^{-1} and 1480 cm^{-1} bands are highlighted in the spectra.

Figure 12. Plot of the ratio of the integrated absorption intensities of the 1560 cm^{-1} and 1480 cm^{-1} bands vs. polymerization time for polypyrrole tubules grown in a 400 nm pore diameter polycarbonate membrane.

Figure 13. UV-Visible-NIR spectra for 30nm diameter polypyrrole fibrils synthesized at three different temperatures.

Figure 14. C1s XPS spectra of (a) 30nm PPy fibrils, and (b) bulk-synthesized PPy.

Figure 15. N1s XPS spectra of (a) 30nm PPy fibrils, and (b) bulk-synthesized PPy.

Table I. Specifications of the Polycarbonate Template Membranes used in these Studies.

Pore diameter (nm)	Pore density [a] (pores/cm^2)	Thickness [b] (μm)
30	6×10^8	6
200	3×10^8	10
400	1×10^8	10
2000	2×10^6	10

[a] From Poretics Corp. product literature.

[b] Measured by using a digital micrometer.

Table II. Conductivities and A_{1560}/A_{1480} for polypyrrole fibrils of various diameters synthesized at room temperature.

Fibril Diameter (nm)	Conductivity ($S\,cm^{-1}$)	A_{1560}/A_{1480}
2000	90	3.15
400	200	2.30
200	625	1.68
30	734	1.52

Table III. Conductivities and A_{1560}/A_{1480} for 30nm polypyrrole fibrils synthesized at different temperatures.

Synthesis Temperature (°C)	Conductivity (S cm^{-1})	A_{1560}/A_{1480}
23	317	2.50
0	923	1.85
-20	2215	0.86

Table IV. Core-level XPS Data for Bulk-Synthesized PPy Powder and 30nm Diameter PPy Fibrils.

	C1s			N1s		
	Position	Area	FWHM	Position	Area	FWHM
	eV	%	eV	eV	%	eV
Powder	283.7	23.2	1.14	397.6	13.9	1.61
	284.9	48.5	1.24	399.6	62.9	1.42
	286.0	18.7	1.34	401.0	15.5	1.21
	287.7	9.7	1.94	402.5	7.8	1.61
Fibrils	284.3	74.8	1.81	397.8	4.6	1.01
	285.9	18.5	1.74	399.8	79.0	1.54
	287.9	6.7	1.74	401.3	12.6	1.18
				402.6	3.8	1.08

Table V. Elemental Analysis Data for Bulk-Synthesized PPy Powder and 30nm Diameter PPy Fibrils.

	C%	H%	N%	Cl%	O%
Powder	57.62	3.63	17.57	9.50	8.37
Fibrils	55.20	3.26	15.90	12.95	8.20
Formula	$C_xN_{1.0}H_yCl_zO_e$				
Powder	$C_{3.8}NH_{2.9}Cl_{0.22}O_{0.42}$				
Fibrils	$C_{4.0}NH_{2.9}Cl_{0.32}O_{0.45}$				

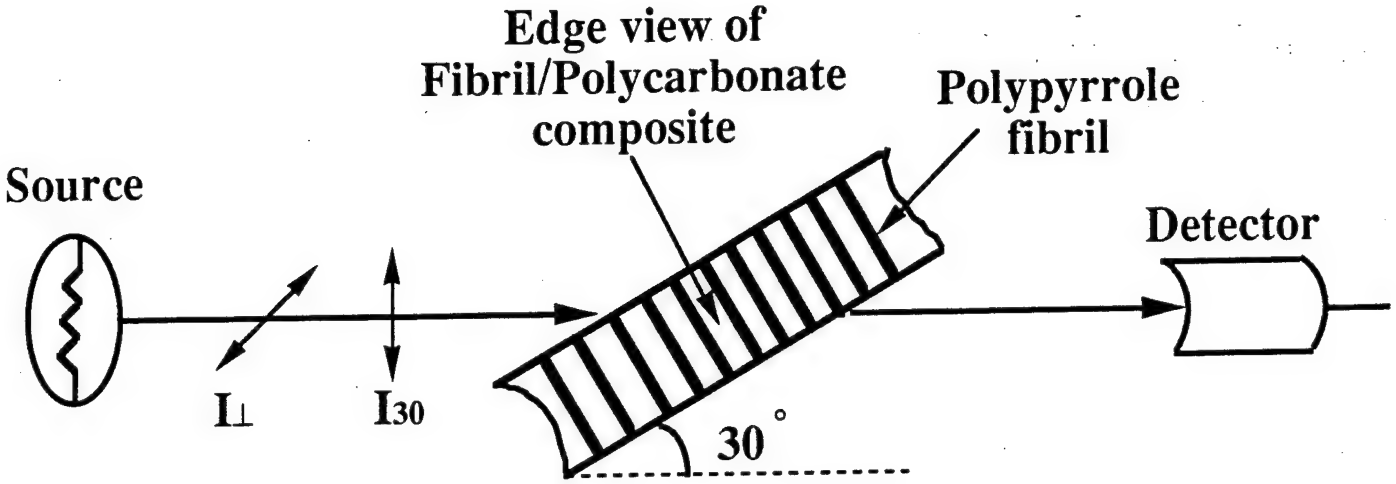
Edge view of
Fibril/Polycarbonate
composite
Polypyrrole
fibril
Source
Detector
I⊥
I30
30°

FIGURE 1

FIGURE 2A

FIGURE 2B

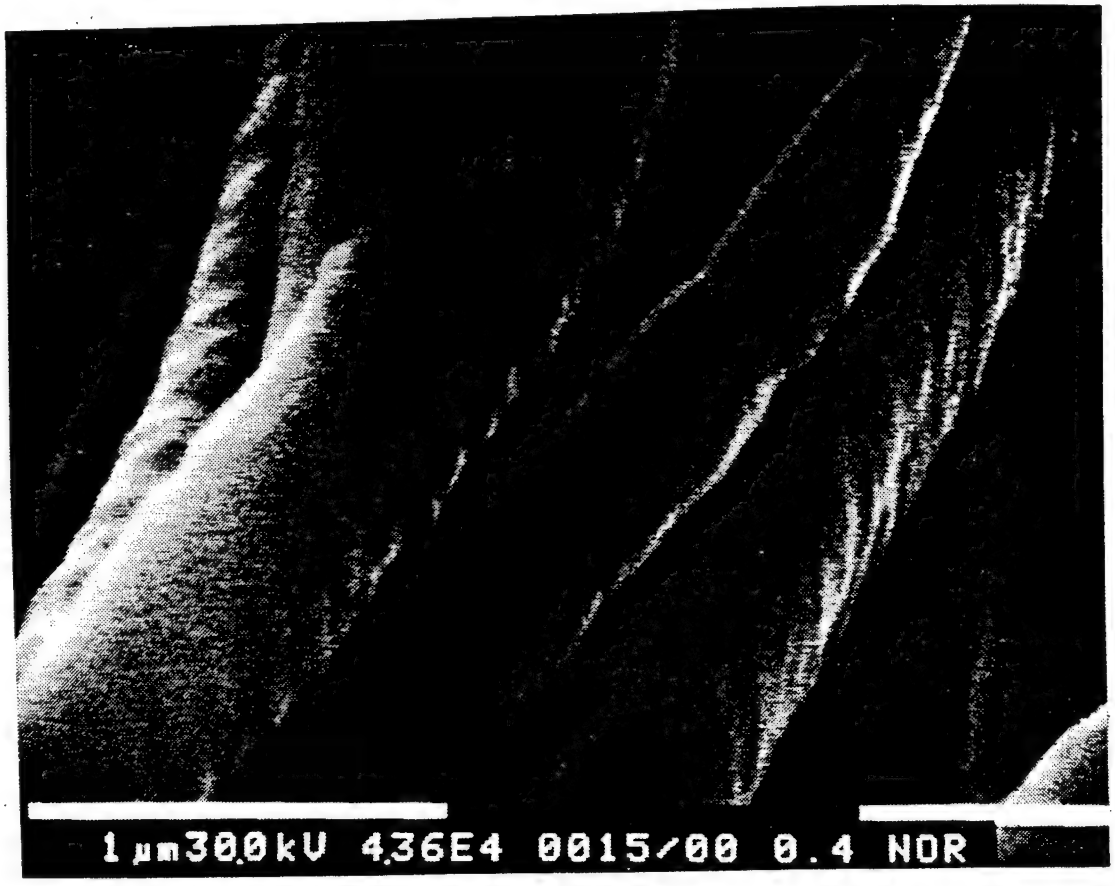

FIGURE 3

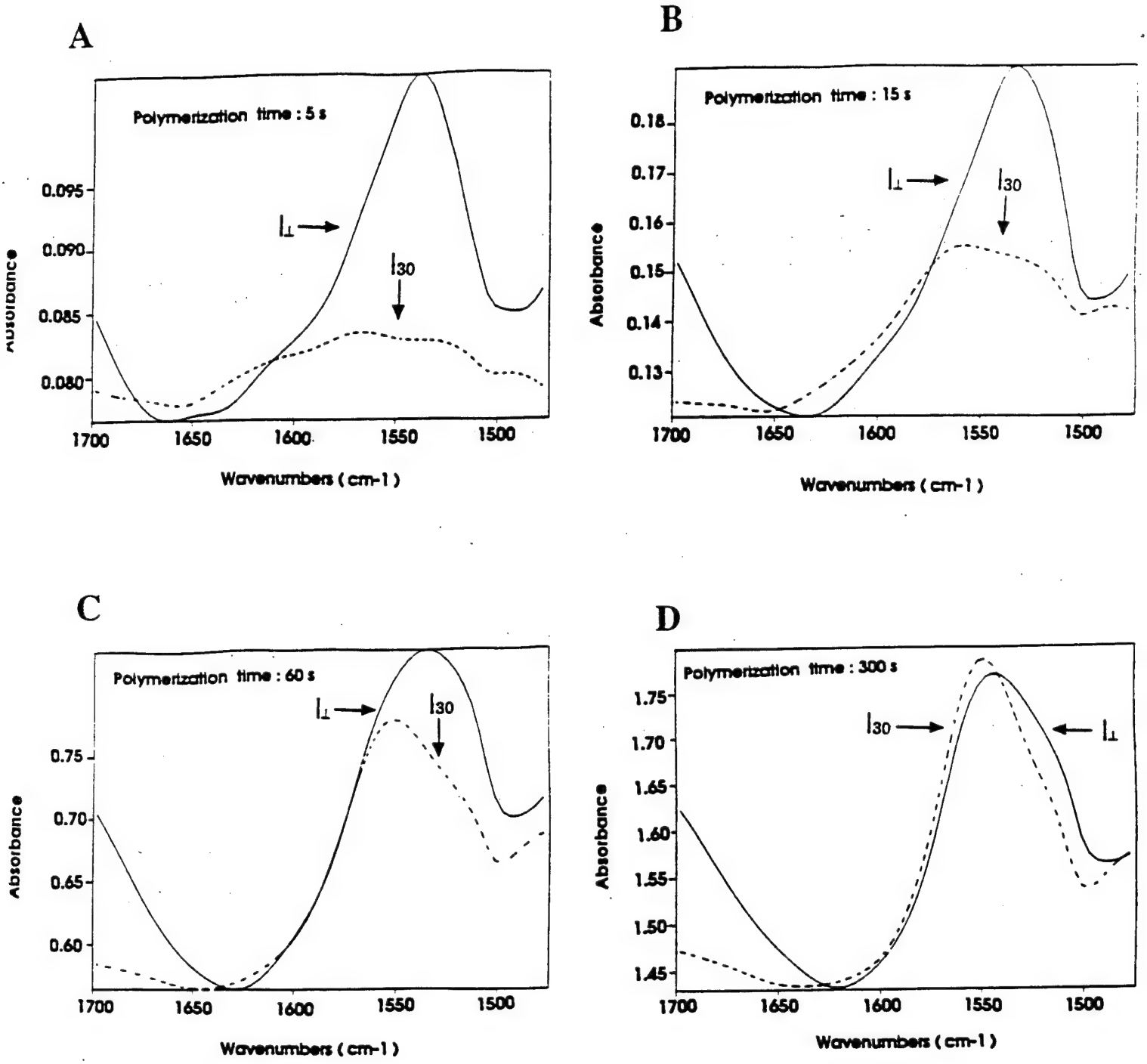
A
Polymerization time : 5 s
0.095
0.090
0.085
0.080
Absorbance
$I_\perp$
I_{30}
1700
1650
1600
1550
1500
Wavenumbers (cm-1)
B
Polymerization time : 15 s
0.18
0.17
0.16
0.15
0.14
0.13
Absorbance
$I_\perp$
I_{30}
1700
1650
1600
1550
1500
Wavenumbers (cm-1)
C
Polymerization time : 60 s
0.75
0.70
0.65
0.60
Absorbance
$I_\perp$
I_{30}
1700
1650
1600
1550
1500
Wavenumbers (cm-1)
D
Polymerization time : 300 s
1.75
1.70
1.65
1.60
1.55
1.50
1.45
Absorbance
I_{30}
$I_\perp$
1700
1650
1600
1550
1500
Wavenumbers (cm-1)

Fig. 4

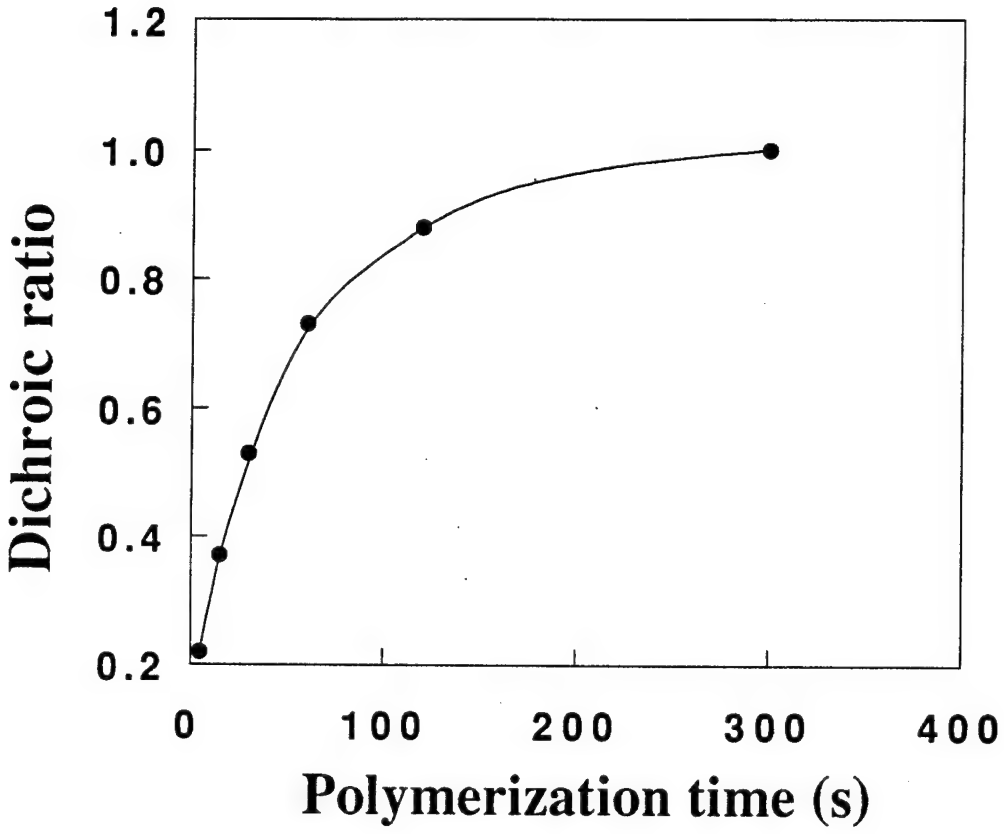
1.2
1.0
0.8
0.6
0.4
0.2
Dichroic ratio
0
100
200
300
400
Polymerization time (s)

FIGURE 5

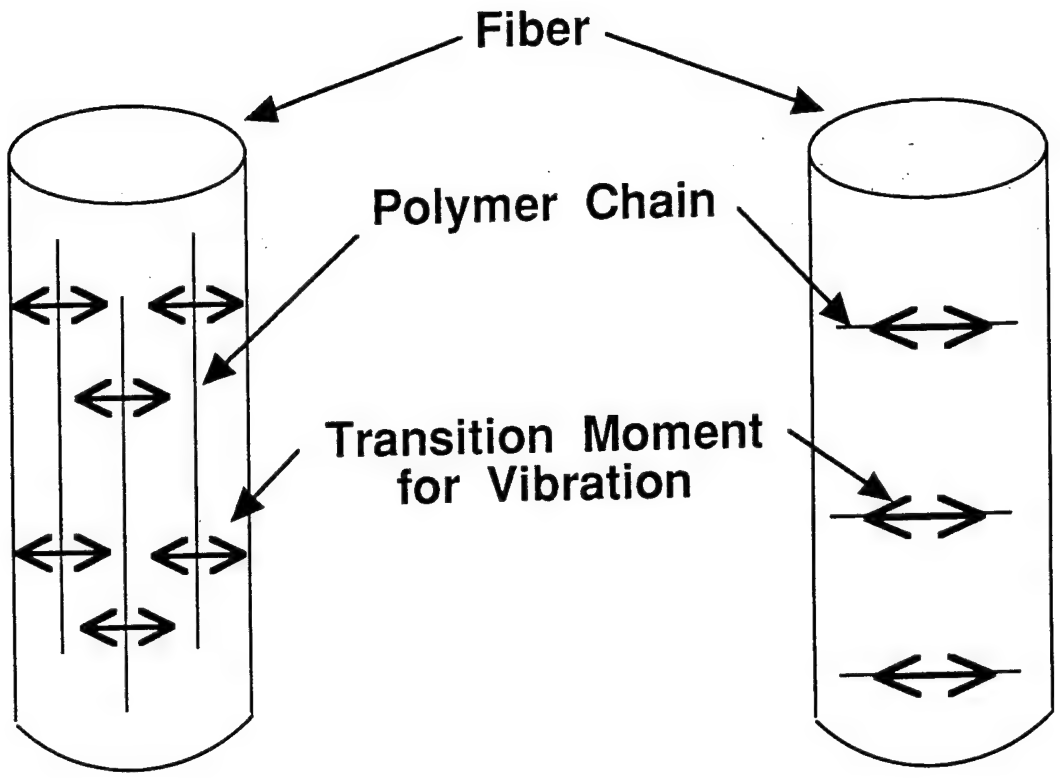

Polymer Chain Parallel.
Transition Moment for
Vibration Perpendicular
to chain.

Polymer Chain Perpendicular.
Transition Moment for
Vibration Parallel to chain.

Fig 6

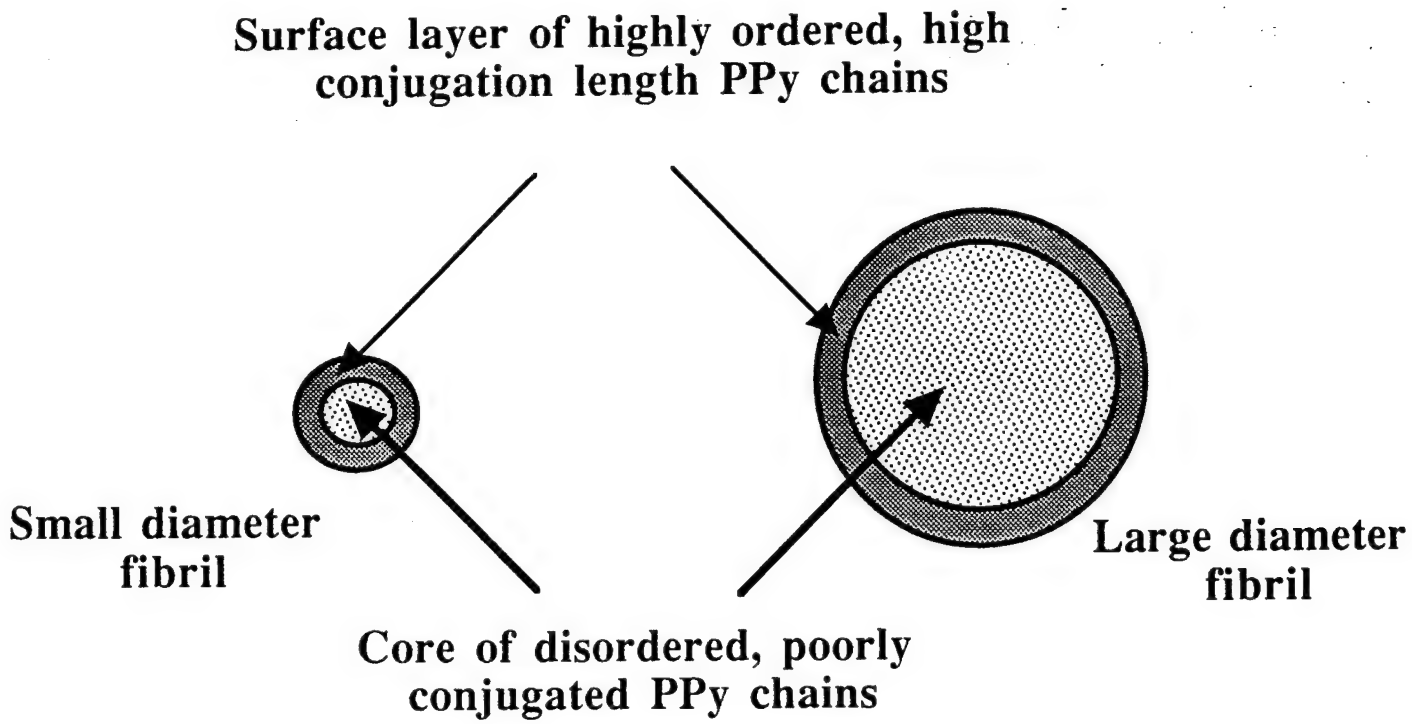
Surface layer of highly ordered, high conjugation length PPy chains
Small diameter fibril
Large diameter fibril
Core of disordered, poorly conjugated PPy chains

Fig 7

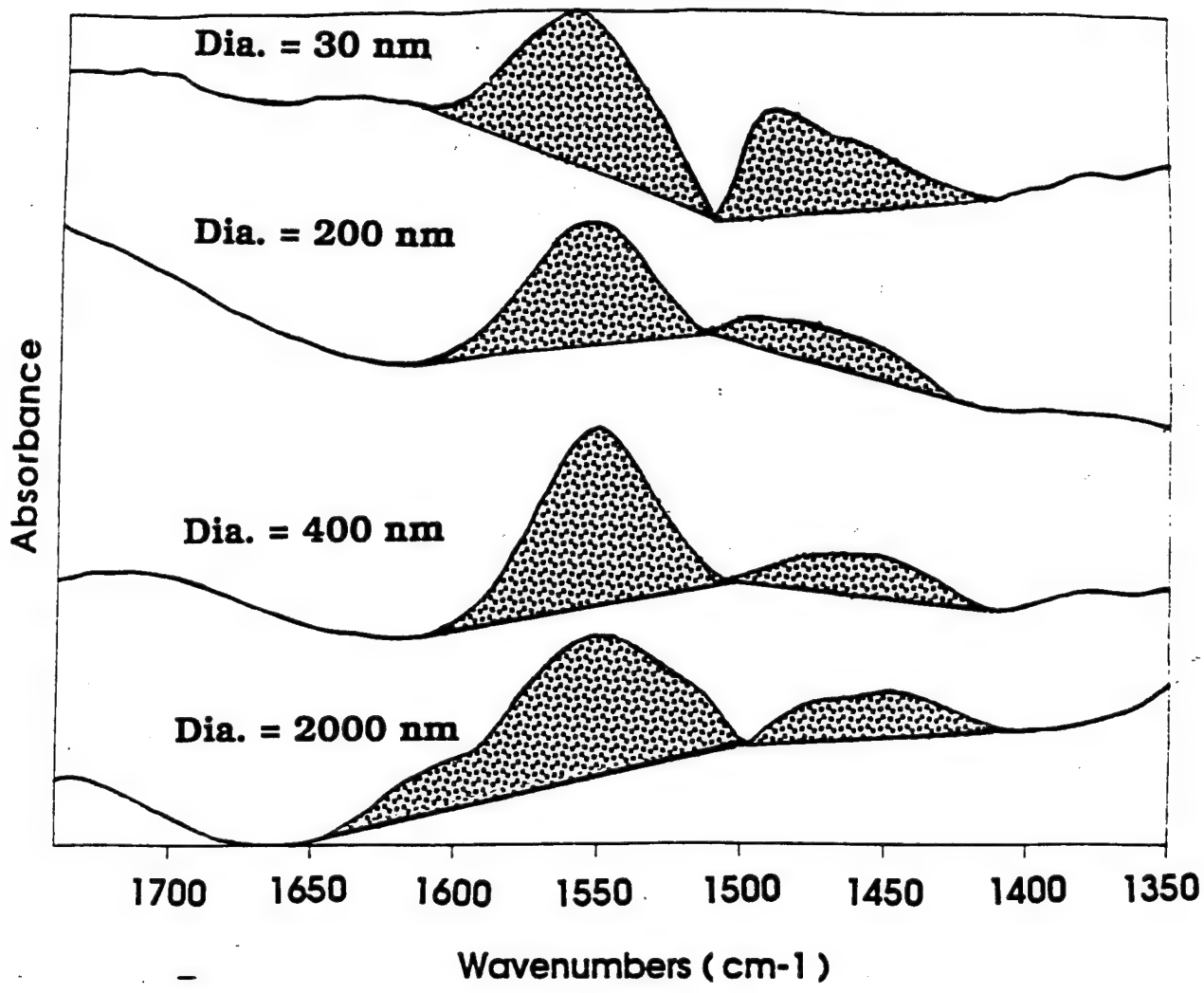
Dia. = 30 nm
Dia. = 200 nm
Dia. = 400 nm
Dia. = 2000 nm
Absorbance
1700
1650
1600
1550
1500
1450
1400
1350
Wavenumbers (cm-1)

FIGURE 8

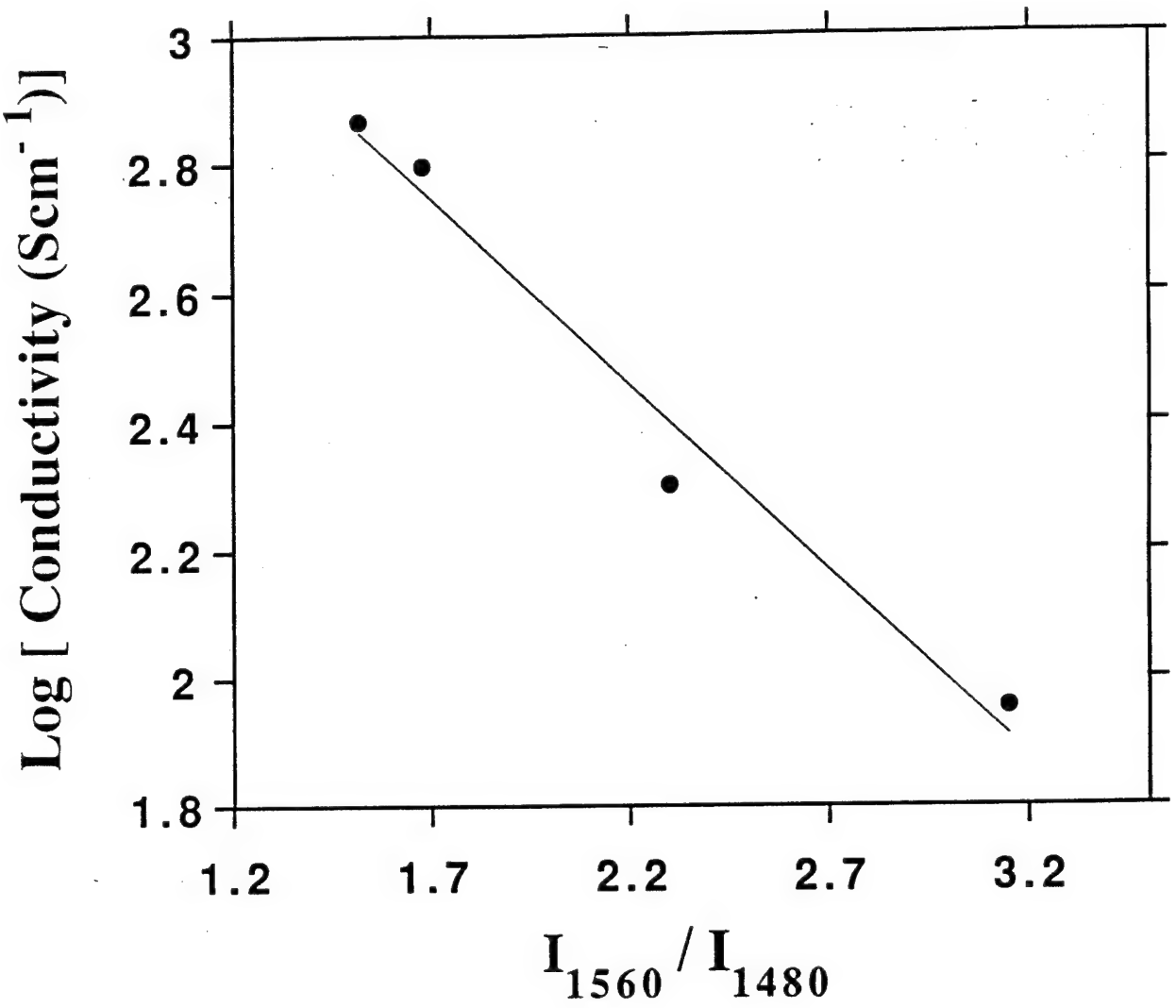
Log [Conductivity (Scm-1)]
3
2.8
2.6
2.4
2.2
2
1.8
1.2
1.7
2.2
2.7
3.2
I1560 / I1480

Fig 9

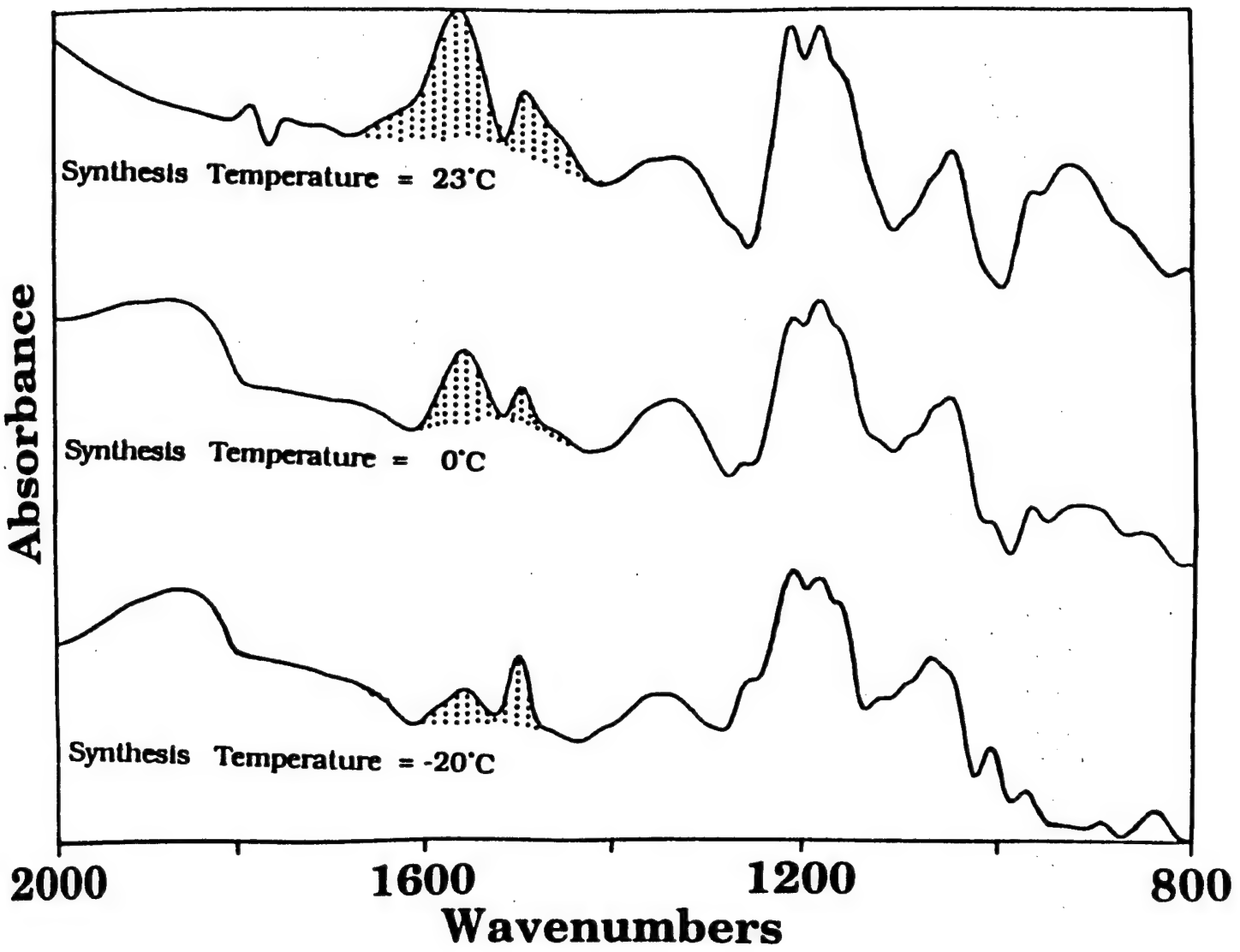
Synthesis Temperature = 23°C
Synthesis Temperature = 0°C
Synthesis Temperature = -20°C
Absorbance
2000
1600
1200
800
Wavenumbers

Fig 5D

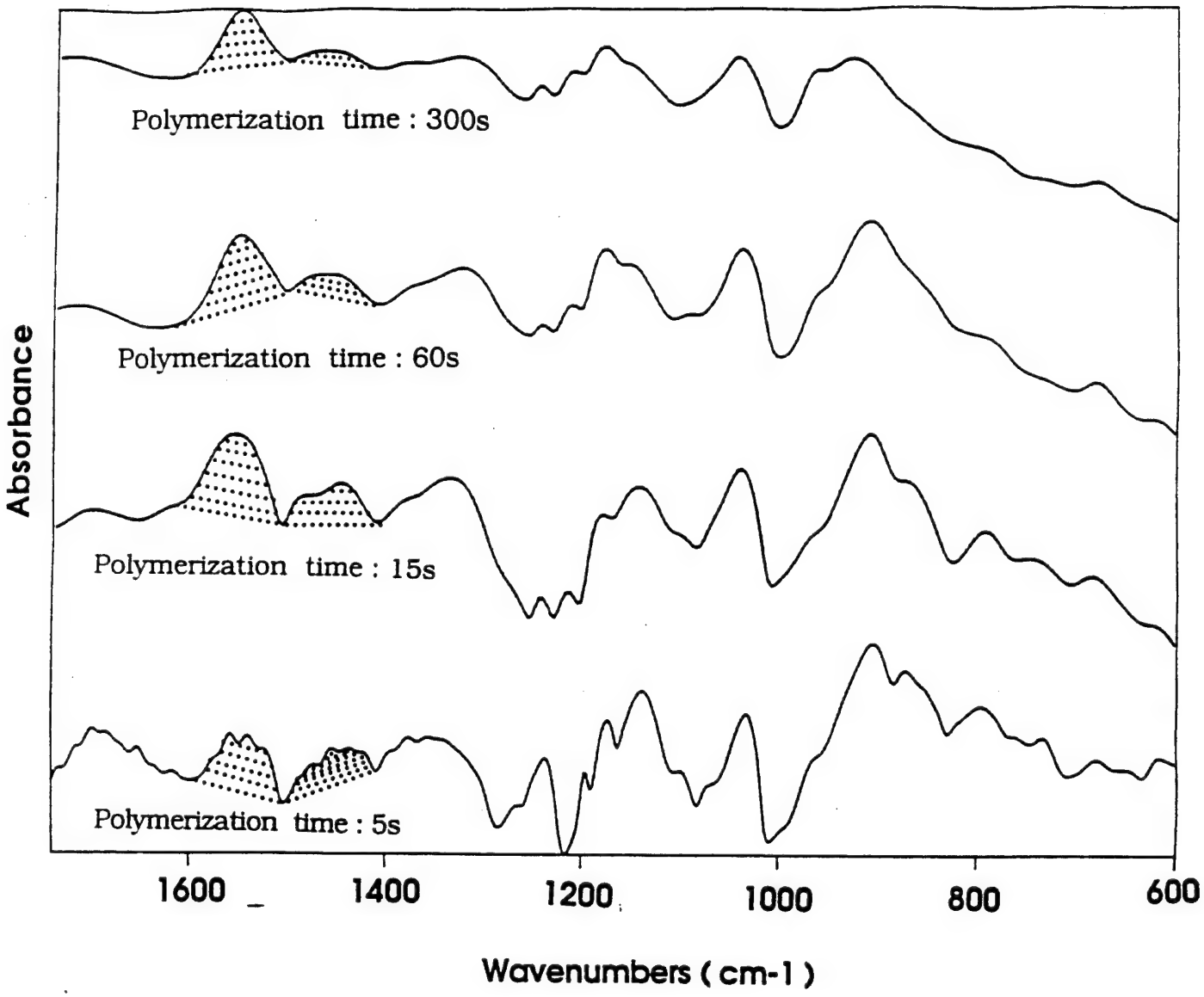
Polymerization time : 300s
Polymerization time : 60s
Polymerization time : 15s
Polymerization time : 5s
Absorbance
1600
1400
1200
1000
800
600
Wavenumbers (cm-1)

Fig 11

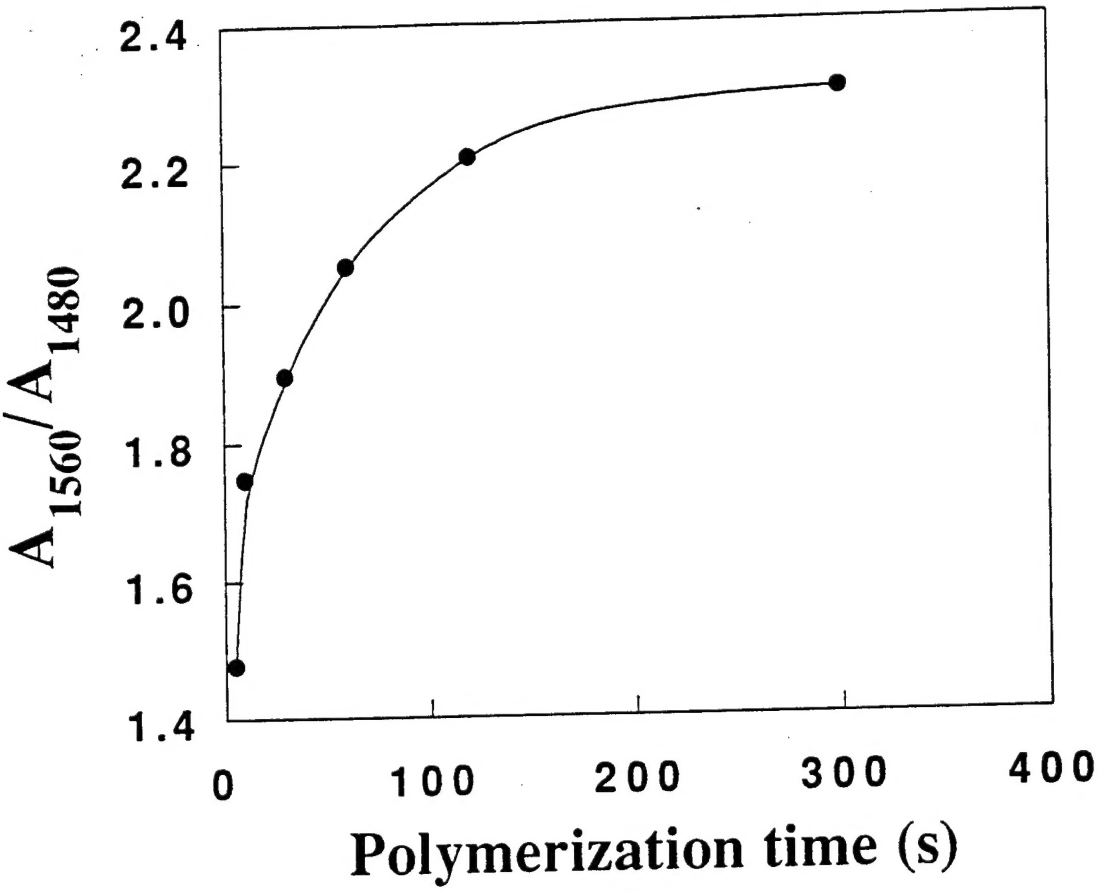
2.4
2.2
2.0
1.8
1.6
1.4
A_{1560}/A_{1480}
0
100
200
300
400
Polymerization time (s)

FIGURE 12

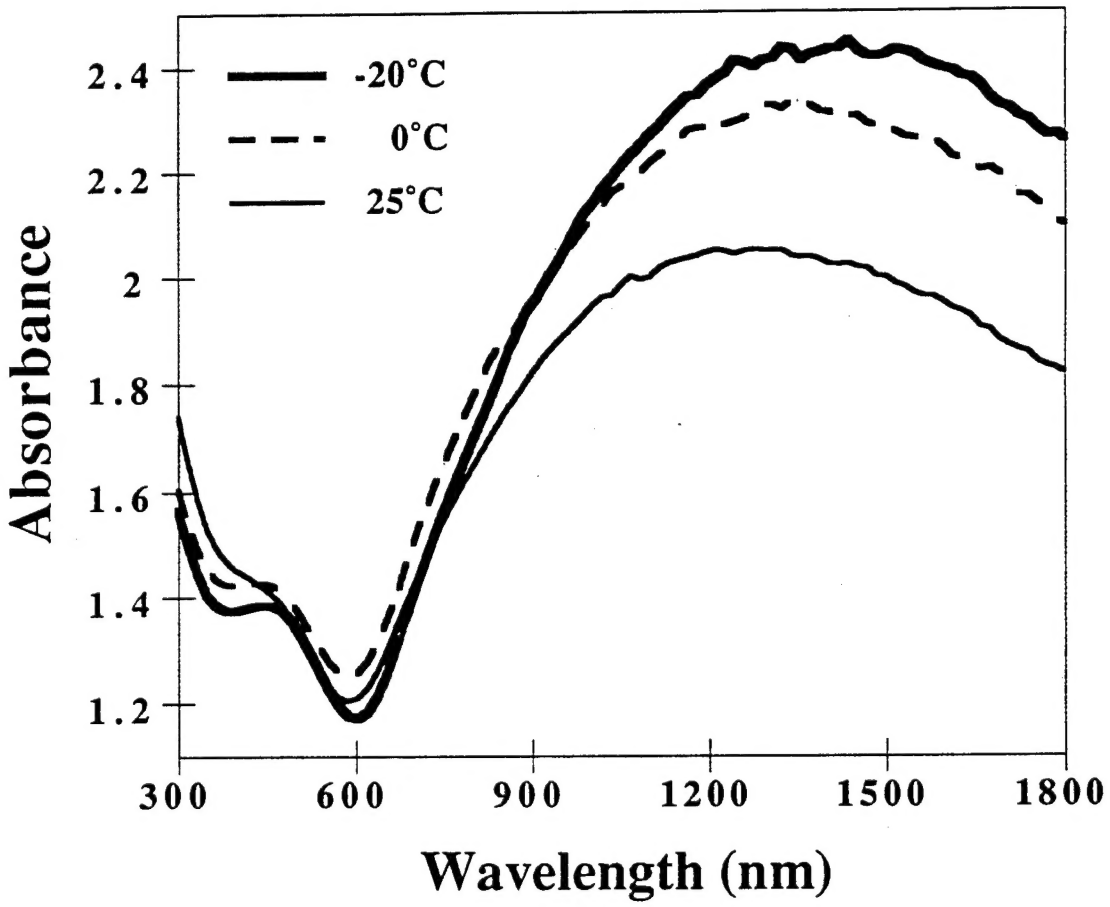
-20°C
0°C
25°C
Absorbance
2.4
2.2
2
1.8
1.6
1.4
1.2
300
600
900
1200
1500
1800
Wavelength (nm)

Fig13

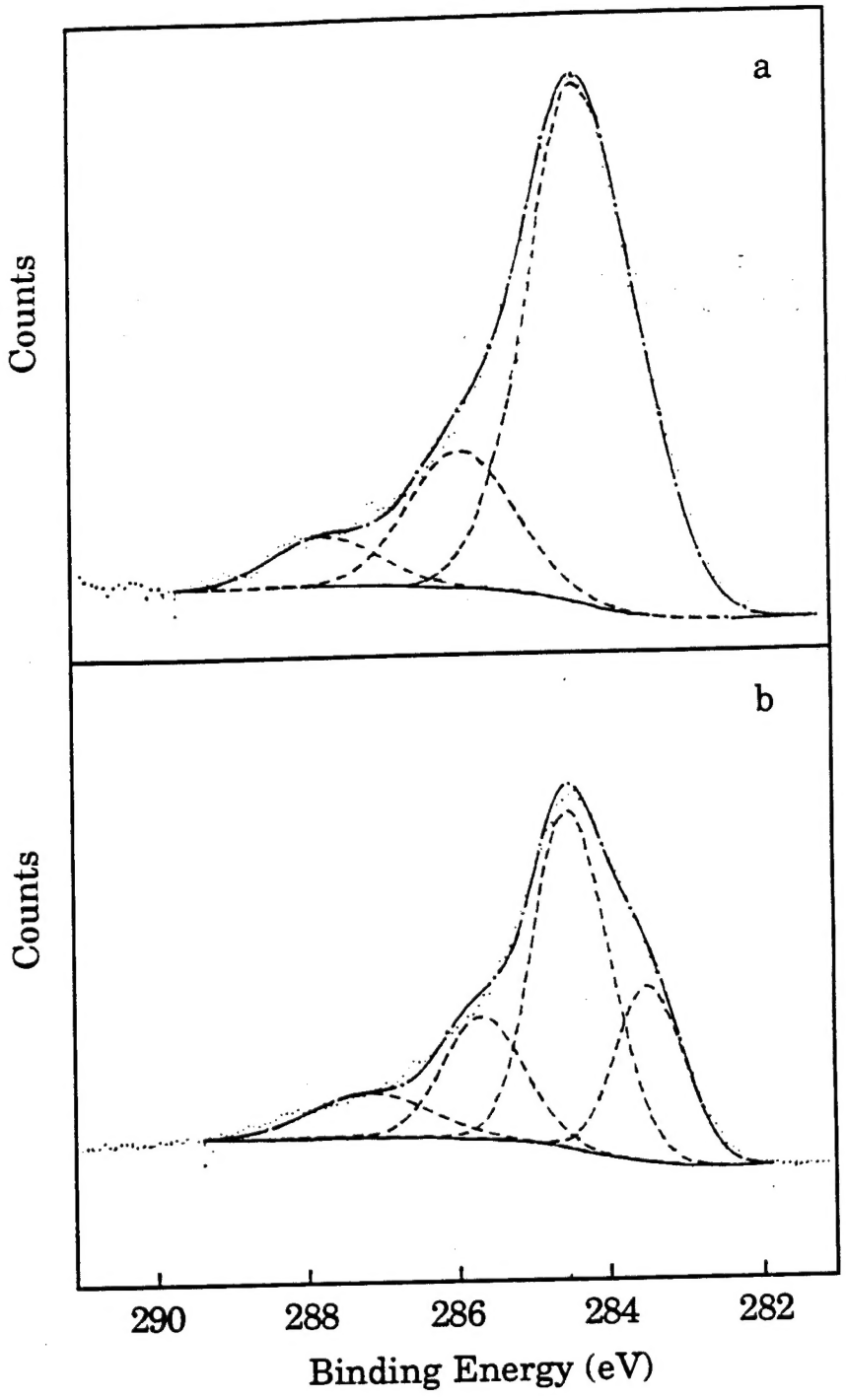

Fig 14

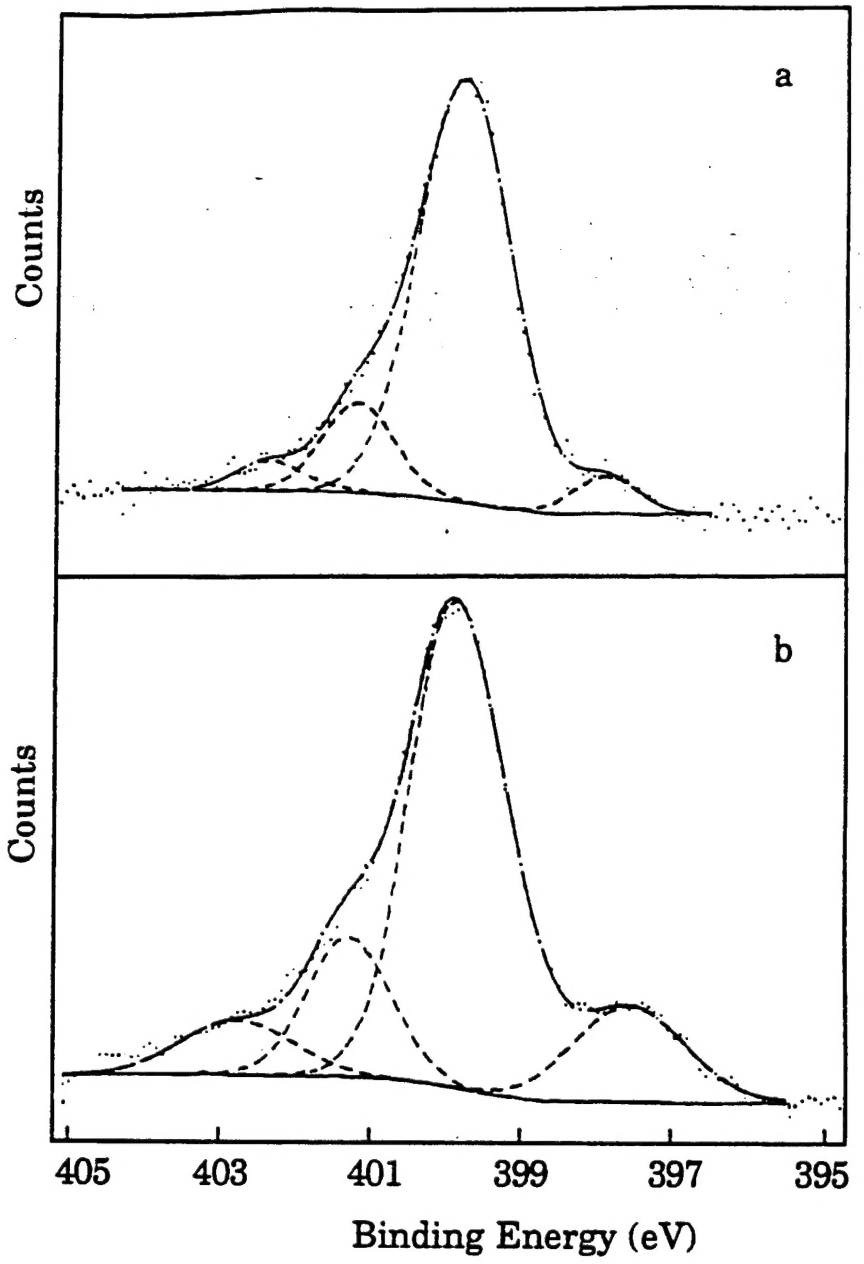

FIGURE 15